Expanded uncertainty regions for complex quantities

B. D. Hall

Measurement Standards Laboratory of New Zealand, Callaghan Innovation, PO Box 31-310, Lower Hutt 5040, New Zealand

E-mail: blair.hall@callaghaninnovation.govt.nz

Abstract. The expanded measurement uncertainty of a complex quantity is a region in the complex plane surrounding the measured value. This paper considers different shaped uncertainty regions in the form of ellipses, circles, rectangles and parallelograms. The different types of region are compared, under a variety of measurement error conditions, with regard to coverage probability and relative area. Elliptical confidence regions are commonly used in multivariate statistics. However, this shape has not been adopted widely in metrology, perhaps because there is no simple way to report the extent of an elliptical region. The other shapes considered are easier to use. Unfortunately, the coverage probability of circular uncertainty regions is found to be sensitive to both the form of the distribution of measurement errors and to the number of degrees of freedom, making this shape a poor choice. Parallelograms and rectangles both performed well, with parallelograms giving the best results overall.

1. Introduction

The expanded measurement uncertainty of a complex quantity is a region in the complex plane surrounding the measured value. The shape of that region is arbitrary, so this article considers using ellipses, circles, rectangles and two forms of parallelogram to report the expanded uncertainty of measurement results expressed in rectangular coordinates.‡ The performance of these uncertainty regions is compared in terms of the coverage probability, or level of confidence, achieved under different measurement error conditions. The study also compares the sizes of the regions generated, because, in cases where different shaped regions achieve close to the desired nominal coverage probability, smaller regions convey more informative results.

An ellipse is often used as a confidence region for the mean of a bivariate Gaussian distribution in multivariate statistics [2, §5.4], making this shape a natural candidate for measurement uncertainty [3]. Unfortunately, the extent of an elliptical region is difficult to report in a simple way. Alternatively, circular and rectangular regions are easy to describe, but do not use in their construction all the uncertainty information available. Parallelograms, on the other hand, do incorporate full uncertainty information in their construction and may therefore be expected to perform better than circles and rectangles in certain circumstances. Numerical studies presented here show that parallogrammatic regions can achieve nominal coverage probability over a wide range of error conditions and are only slightly larger than the corresponding uncertainty ellipses.

Reporting of expanded uncertainties is common for measurements of real-valued quantities. However, to the author's knowledge, only one national metrology institute currently uses a region to report the measurement uncertainty of a complex quantity [4]. More often, the components of a complex quantity are reported as expanded uncertainty intervals calculated according to the recommendations of the *Guide to the Expression of Uncertainty in Measurement* for univariate results [5]. However, this is only appropriate if the results are to be treated as independent estimates of univariate quantities. If, for example, a pair of 95% uncertainty intervals for the real and imaginary components were to be combined to form a rectangular region for the complex quantity, the coverage probability of that region would only be about 90%.

The convenience of a particular shape of uncertainty region may depend on the intended use of results. For instance, in the context of radio and microwave frequency impedance measurements, the complex-valued properties of a number of stable reference objects (sometimes called a verification kit) may be carefully measured by a calibration laboratory. The owner can then use the same objects to verify that a measuring instrument is operating correctly, by comparing the reported values with measurements of the objects made on the instrument. If the differences between reported and measured values fall within an acceptable tolerance region, then the instrument's adjusted state is verified. In such cases, the extent of the region should be presented in a way that can

‡ Uncertainty regions for complex quantities expressed in polar coordinates are the subject of another paper [1].

easily compared with measured values.

The geometric simplicity of circular uncertainty regions is appealing. Unfortunately, a recent study has identified problems with the coverage probability of circular regions when measurement errors are correlated [6]. Circular regions may also be attractive because of a simple method for evaluating complex uncertainty, based on the assumption of independent and equal error-variances in the real and imaginary components [7]. This method is easier to apply than the mathematical techniques needed for full bivariate uncertainty propagation and it produces results that may be expressed in terms of circular uncertainty regions.

Supplement 2 to the *Guide to the Expression of Uncertainty in Measurement* describes the construction of both elliptical and rectangular uncertainty regions when degrees of freedom are infinite [8, §6.5.2.3]. To handle finite degrees of freedom, the Supplement proposes a numerical Monte Carlo method that, if used to construct elliptical uncertainty regions, would lead to the essentially the same elliptical regions considered here.

The paper is organised as follows. A numerical method used to assess the coverage probability of different shapes is described in §1.3 and §1.4. Sections 2, 3, 4 and 5 then present, respectively, the construction of ellipses, circles, rectangles and parallelograms as uncertainty regions and evaluate their performance. The results are discussed in §6.

1.1. Notation

Real-valued quantities are written in plain italic font, like x. Complex-valued quantities are written in bold italic font, like $\boldsymbol{x}$. Greek characters are written in plain style when representing real values and in bold when representing a complex values, e.g., ν and $\boldsymbol{\mu}$. Symbols representing matrices are written in bold upright font, like $\mathbf{v}$. The imaginary unit j, where $\mathrm{j}^2 = -1$, is used, e.g., $\boldsymbol{x} = x_{\mathrm{re}} + \mathrm{j}\, x_{\mathrm{im}}$ (note too, the use of subscript labels identifying the real and imaginary components).

1.2. Information available about uncertainty

The uncertainty of the measured value of a complex quantity depends on the measurement uncertainty of the real and imaginary components and on any correlation between those estimates. A covariance matrix is a convenient representation of this information

$$\mathbf{v} = \begin{bmatrix} v_{11} & v_{12} \\ v_{21} & v_{22} \end{bmatrix},$$

where $v_{11} = u^2(x_{\mathrm{re}})$, with $u(x_{\mathrm{re}})$ the standard uncertainty of the real component estimate, $v_{22} = u^2(x_{\mathrm{im}})$, with $u(x_{\mathrm{im}})$ the standard uncertainty of the imaginary component estimate, and $v_{12} = v_{21}$ is the covariance between the estimates ($v_{21} = ru(x_{\mathrm{re}})u(x_{\mathrm{im}})$, where r is the correlation coefficient).

Covariance matrix elements can be calculated from a sample of N observations $\boldsymbol{x}_i$ as follows. The sample mean is

$$\overline{\boldsymbol{x}} = \overline{x}_{\mathrm{re}} + \mathrm{j}\,\overline{x}_{\mathrm{im}} = \frac{1}{N}\left[\sum_{i=1}^{N} x_{i\cdot\mathrm{re}} + \mathrm{j}\,\sum_{i=1}^{N} x_{i\cdot\mathrm{im}}\right]$$

then

$$v_{11} = \frac{1}{N(N-1)}\sum_{i=1}^{N}\left(x_{i\cdot\mathrm{re}} - \overline{x}_{\mathrm{re}}\right)^2$$

and

$$v_{22} = \frac{1}{N(N-1)}\sum_{i=1}^{N}\left(x_{i\cdot\mathrm{im}} - \overline{x}_{\mathrm{im}}\right)^2$$

and the covariance is

$$v_{12} = v_{21} = \frac{1}{N(N-1)}\sum_{i=1}^{N}\left(x_{i\cdot\mathrm{re}} - \overline{x}_{\mathrm{re}}\right)\left(x_{i\cdot\mathrm{im}} - \overline{x}_{\mathrm{im}}\right) \ .$$

The number of degrees of freedom associated with the sample is $\nu = N - 1$.

The covariance matrix of a measurement result may also be obtained by propagation of uncertainty through a measurement equation [3, 8, 9]. In that case, a method of calculating an effective number of degrees of freedom is also available [10].

1.3. Assessment of coverage probability

A numerical procedure is used to estimate the coverage probability, or level of confidence, for different methods of constructing an uncertainty region. Coverage probability is taken to be the long-run relative frequency, in independent measurements, that a procedure generates regions covering the measurand [11]. This can be assessed by simulating a large number of independent measurements and observing the relative frequency with which regions cover the measurand in a well-defined situation [12].

The simulations carried out in this study test a method of uncertainty calculation under a range of specific conditions, whereas in actual measurements the conditions encountered will never be known exactly. Nevertheless, we expect a method of calculating uncertainty to perform well under all conditions that could occur in a measurement. So poor performance under any reasonable set of simulated conditions must be of concern.

To define a specific set of measurement conditions, a number of simulation parameters are fixed: the degrees of freedom ν, the covariance matrix of the underlying distribution of measurement errors $\boldsymbol{\Sigma}$ and the measurand $\boldsymbol{\mu}$. Without loss of generality, $\mu = 0$ here in all cases. The simulation algorithm for a particular method of constructing an uncertainty region repeats the following steps $N = 10^5$ times and records the success-rate.

(i) A random value is drawn from a bivariate Gaussian distribution with a mean of $\boldsymbol{\mu} = 0$ and a covariance matrix Σ. The value drawn is considered to be the outcome of a simulated measurement of μ.

(ii) A random 2×2 matrix $\mathbf{v}_i$ is drawn from a two-dimensional Wishart distribution with covariance matrix Σ and degrees of freedom ν. $\mathbf{v}_i$ is associated with the uncertainty of $\boldsymbol{x}_i$ as an estimate of μ.

(iii) Together, $\boldsymbol{x}_i$, $\mathbf{v}_i$ and ν are used to construct an uncertainty region with a nominal coverage probability of 95%.

(iv) If that region covers $\boldsymbol{\mu}$, the calculation is deemed a 'success'.

The success-rate obtained provides an estimate of the coverage probability. The standard deviation of this estimate can be calculated by assuming a binomial probability distribution of outcomes. For a probability of success $p = 0.95$ and $N = 10^5$, $\sigma = \sqrt{p(1-p)N} \approx 69$ or about 0.07%. So, the uncertainty in the observed success-rate, as an estimate of the actual coverage probability, is about 0.14% (at approximately 95% confidence level).

To investigate a method's performance under different conditions, simulations have been carried out with different Σ and ν. The covariance matrix was parameterised as follows

$$\Sigma = \begin{bmatrix} 1 & \rho l \\ \rho l & l^2 \end{bmatrix} ,$$

with $\rho = 0.0, 0.2, 0.5, 0.8$ and the standard uncertainty of the imaginary component $l = 1.0, 2.0, 4.0, 8.0$. The degrees of freedom $\nu = 3, 5, 10, 50, \infty$.

1.4. Area as an additional performance measure

If two methods of calculating an uncertainty perform well in terms of coverage probability, then the size of the uncertainty regions should be compared. Smaller regions are desirable, because they are more informative about the location of the measurand. For instance, if the areas of uncertainty regions generated by method 'A' are consistently smaller than those generated by method 'B', while both methods achieve a satisfactory coverage probability, then method 'A' would be preferred.

With this in mind, we have also recorded the mean area of the regions being studied relative to the mean area of elliptical regions calculated from the same data.

2. Uncertainty ellipses

An ellipse is a commonly used confidence region for the mean of a bivariate Gaussian distribution [2, Ch. 5]. An elliptical region may be expressed as the locus of points $\boldsymbol{\xi}$ that satisfy

$$(\boldsymbol{\xi} - \boldsymbol{x})' \, \mathbf{v}^{-1} \, (\boldsymbol{\xi} - \boldsymbol{x}) \leq k^2_{\mathrm{ell},p} \, , \tag{1}$$

where $k^2_{\mathrm{ell},p}$ is a coverage factor (squared) that scales the area of the region to achieve a coverage probability p

$$k^2_{\mathrm{ell},p}(\nu) = \frac{2\nu}{\nu - 1} F_{2,\nu-1}(p) \; , \tag{2}$$

$F_{2,\nu-1}(p)$ is the upper $100p^{\mathrm{th}}$ percentile of the F-distribution with numerator parameter 2 and denominator parameter $\nu - 1$.

To determine whether a point $\boldsymbol{\xi}$ lies inside an elliptical uncertainty region centered on $\boldsymbol{x}$ with a covariance matrix $\mathbf{v}$, the Mahalanobis distance can be calculated

$$d(\boldsymbol{\xi}) = \sqrt{(\boldsymbol{\xi} - \boldsymbol{x})' \; \mathbf{v}^{-1} \; (\boldsymbol{\xi} - \boldsymbol{x})} \tag{3}$$

and if $d(\boldsymbol{\xi}) \leq k_{\mathrm{ell},p}$, then $\boldsymbol{\xi}$ is within the uncertainty region. The calculation required to determine whether two ellipses overlap, and if so by how much, is rather more complicated. So, in terms of reporting, it is probably best to directly record the covariance matrix elements and the number of degrees of freedom, or coverage factor, leaving the formulation of any calculations required to the recipient of a report.

2.1. Performance

No simulation results are presented in this section, because equation (1) describes the construction of a confidence region for the mean of a bivariate Gaussian distribution in classical statistics, and is exact [2]. For that reason, the success-rates obtained from simulations would only differ from the nominal coverage probability because of the inherent variability due to the finite number of simulations.

3. Uncertainty circles

In an alternative expression of equation (1),

$$\frac{(x_{\mathrm{re}} - \xi_{\mathrm{re}})^2}{v_{11}} + \frac{(x_{\mathrm{im}} - \xi_{\mathrm{im}})^2}{v_{22}} - 2v_{21} \frac{(x - \xi_{\mathrm{re}})}{\sqrt{v_{11}}} \frac{(y - \xi_{\mathrm{im}})}{\sqrt{v_{22}}} = k^2_{\mathrm{ell},p} \; , \tag{4}$$

we see that when $v_{21} = 0$ the principal axes of the ellipse lie parallel to the real and imaginary coordinate axes and when the uncertainties of the real and imaginary components are equal ($v_{11} = v_{22}$) the region becomes a circle. So, circular uncertainty regions may be appropriate when the variance of measurement errors in the real and imaginary components is approximately equal and the errors are independent.

Uncertainty circles were suggested some time ago and appear to be the only type of region currently used to report the expanded uncertainty of complex quantities [4]. Only the radius and level of confidence need be recorded, which makes reporting no more complicated than for real-valued quantities. However, this reporting format provides insufficient information to recover the covariance matrix elements, should they be needed for further uncertainty calculations.

A circular uncertainty region with nominal coverage probability p can be constructed by ignoring the covariance element and averaging the diagonal elements of the covariance matrix. The circle radius is then

$$R = k_{\mathrm{ell},p} \sqrt{\frac{v_{11} + v_{22}}{2}} \,. \tag{5}$$

This circle has a simple geometric interpretation. It has an area equal to the mean area of the inscribing and circumscribing circles of the uncertainty ellipse, as shown in Fig. 1.

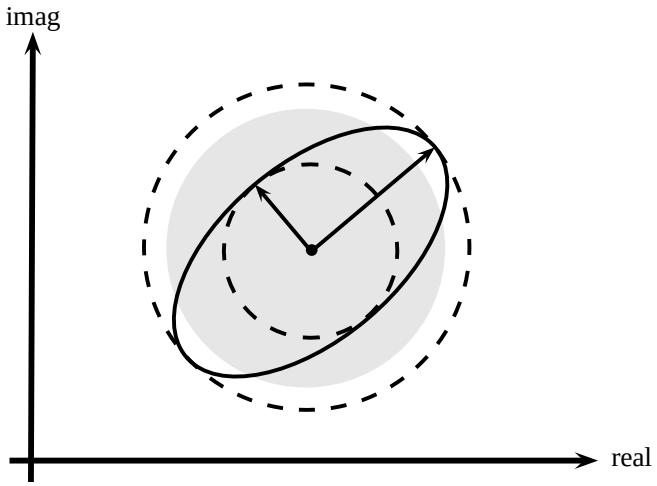

Figure 1. The area of the grey uncertainty region is the mean area of the inscribed and circumscribed circles (dashed). The major and minor ellipse axes align with the covariance matrix eigenvectors. The lengths of these axes are proportional to the square root of the corresponding eigenvalues.

3.1. Performance

Table 1 shows the estimated coverage probabilities for circular uncertainty regions. The observed success rates are close nominal when degrees of freedom are high and errors in the real and imaginary components are of similar magnitude. However, if errors in the real and imaginary components are of different magnitudes, or if there is significant correlation between them, the coverage probability drops below nominal when $\nu > 10$. Under the same conditions (l and ρ the same), coverage probability rises with decreasing ν and so when errors in the real and imaginary components are of similar magnitude coverage probabilities can be seen to rise significantly above nominal.

The mean area ratios are never less than unity, indicating that circle areas are, on average, at least as big as the uncertainty ellipses, even when coverage probability drops below nominal. When the coverage probability is well above nominal, the mean area ratios data shows that the circles can become quite a lot larger than the equivalent ellipses.

A drop in coverage probability of several percentage points below nominal is unlikely to be acceptable, so a more conservative circular construction has also been

		success-rate				mean area ratio			
ν	l	$\rho = 0.0$	0.2	0.5	0.8	$\rho = 0.0$	0.2	0.5	0.8
500	1	0.9512	0.9497	0.9413	0.9266	1.00	1.02	1.16	1.67
	2	0.9357	0.9355	0.9330	0.9235	1.25	1.28	1.45	2.09
	4	0.9227	0.9235	0.9216	0.9194	2.13	2.17	2.46	3.55
	8	0.9180	0.9189	0.9194	0.9182	4.07	4.16	4.70	6.78
50	1	0.9573	0.9549	0.9466	0.9333	1.02	1.04	1.18	1.70
	2	0.9433	0.9414	0.9373	0.9301	1.28	1.30	1.47	2.13
	4	0.9296	0.9278	0.9261	0.9249	2.17	2.21	2.50	3.61
	8	0.9239	0.9254	0.9248	0.9248	4.15	4.23	4.78	6.91
10	1	0.9793	0.9779	0.9704	0.9563	1.11	1.13	1.28	1.85
	2	0.9662	0.9643	0.9607	0.9520	1.39	1.42	1.60	2.31
	4	0.9516	0.9532	0.9519	0.9480	2.36	2.41	2.73	3.93
	8	0.9464	0.9468	0.9473	0.9470	4.52	4.61	5.20	7.54
5	1	0.9931	0.9932	0.9890	0.9795	1.25	1.28	1.44	2.08
	2	0.9872	0.9862	0.9825	0.9774	1.56	1.60	1.80	2.60
	4	0.9751	0.9759	0.9742	0.9703	2.66	2.71	3.07	4.42
	8	0.9702	0.9694	0.9700	0.9697	5.09	5.17	5.88	8.47
3	1	0.9992	0.9991	0.9985	0.9966	1.50	1.53	1.73	2.49
	2	0.9982	0.9980	0.9971	0.9948	1.87	1.92	2.16	3.12
	4	0.9943	0.9942	0.9931	0.9911	3.18	3.25	3.69	5.32
	8	0.9898	0.9895	0.9893	0.9889	6.10	6.24	7.06	10.2

Table 1. Observed success-rates for uncertainty circles with radii calculated using equation (5) and the ratio of mean area to the mean area of elliptical regions. The uncertainty in success-rates as estimates of coverage probability is approximately 0.0014.

studied. A circle circumscribing the uncertainty ellipse is guaranteed to provide coverage probabilities that are never less than nominal.§ The radius of that circle is

$$R_{\max} = k_{\mathrm{ell},p}\,\sqrt{\max(\lambda_1, \lambda_2)}\,, \tag{6}$$

where λ_1, λ_2 are the eigenvalues of the covariance matrix $\mathbf{v}$. Table 2 shows the results obtained with these regions. As expected, the coverage probability now stays above 95%. However, the circle areas are considerably larger than the equivalent uncertainty ellipses.

4. Uncertainty rectangles

A rectangular uncertainty region with sides parallel to the real and imaginary coordinate axes can be reported as a pair of simultaneous uncertainty intervals for the real and

§ The locus of points covered by the enclosed ellipse is enough to achieve nominal coverage probability.

		success-rate				mean area ratio			
ν	l	$\rho = 0.0$	0.2	0.5	0.8	$\rho = 0.0$	0.2	0.5	0.8
500	1	0.9583	0.9713	0.9821	0.9851	1.06	1.23	1.74	3.01
	2	0.9839	0.9832	0.9836	0.9851	2.01	2.07	2.49	3.92
	4	0.9851	0.9849	0.9847	0.9856	4.01	4.10	4.70	6.95
	8	0.9854	0.9857	0.9853	0.9856	8.02	8.19	9.29	13.5
50	1	0.9729	0.9769	0.9827	0.9854	1.20	1.31	1.78	3.07
	2	0.9842	0.9838	0.9850	0.9857	2.05	2.12	2.55	4.00
	4	0.9855	0.9846	0.9858	0.9860	4.09	4.18	4.80	7.08
	8	0.9855	0.9857	0.9853	0.9863	8.16	8.34	9.46	13.7
10	1	0.9926	0.9926	0.9900	0.9883	1.54	1.61	2.03	3.38
	2	0.9895	0.9896	0.9882	0.9879	2.30	2.37	2.81	4.37
	4	0.9888	0.9883	0.9886	0.9884	4.48	4.58	5.25	7.74
	8	0.9881	0.9882	0.9880	0.9884	8.89	9.10	10.3	15.0
5	1	0.9983	0.9980	0.9965	0.9934	1.92	1.98	2.40	3.85
	2	0.9959	0.9958	0.9947	0.9928	2.68	2.76	3.24	4.96
	4	0.9926	0.9922	0.9925	0.9912	5.06	5.18	5.94	8.70
	8	0.9913	0.9911	0.9910	0.9912	10.0	10.3	11.6	16.9
3	1	0.9999	0.9997	0.9996	0.9988	2.50	2.57	3.04	4.71
	2	0.9994	0.9993	0.9992	0.9980	3.36	3.42	3.98	6.01
	4	0.9983	0.9977	0.9974	0.9963	6.15	6.30	7.16	10.5
	8	0.9964	0.9963	0.9963	0.9957	12.0	12.3	14.0	20.3

Table 2. Estimated coverage probabilities for uncertainty circles that circumscribe an uncertainty ellipse and the ratio of mean circle area to the mean area of elliptical regions. The uncertainty in the estimates is approximately 0.0014.

imaginary components. It is then a simple matter to determine whether a complex value is covered by a region, or whether two rectangular regions overlap and, if so, by how much.

A rectangular region circumscribing an elliptical uncertainty region would be sure to provide at least nominal coverage probability. However, using the Bonferroni inequality a smaller region can be constructed that still achieves no less than nominal coverage probability [2, §5.4]. The sides of such a rectangle are calculated using a coverage factor

$$k_{\mathrm{B},p} = t_\nu(\alpha) \ ,$$

where $\alpha = (3 + p)/4$ and $t_\nu(\alpha)$ is the $100\alpha^{\mathrm{th}}$ percentile of Student's t-distribution with ν degrees of freedom.‖

For a measured value $\boldsymbol{x}$, with standard uncertainties $u(x_{\mathrm{re}})$ and $u(x_{\mathrm{im}})$, the

‖ Tables of univariate coverage factors can be used to find values for $k_{\mathrm{B},p}$ by looking up a coverage factor for ν and $p' = (1 + p)/2$. For example, $k_{\mathrm{B},95} = 2.248$ when $\nu = 500$ and $k_{\mathrm{B},95} = 4.177$ when $\nu = 3$.

uncertainty rectangle covers all complex values $\boldsymbol{\xi}$ where

$$\xi_{\mathrm{re}} \in [x_{\mathrm{re}} - k_{\mathrm{B},p}u(x_{\mathrm{re}}), x_{\mathrm{re}} + k_{\mathrm{B},p}u(x_{\mathrm{re}})] \tag{7}$$

and simultaneously

$$\xi_{\mathrm{im}} \in [x_{\mathrm{im}} - k_{\mathrm{B},p}u(x_{\mathrm{im}}), x_{\mathrm{im}} + k_{\mathrm{B},p}u(x_{\mathrm{im}})] \; . \tag{8}$$

4.1. Performance

		success-rate				mean area ratio			
ν	l	$\rho = 0.0$	0.2	0.5	0.8	$\rho = 0.0$	0.2	0.5	0.8
500	1	0.9498	0.9511	0.9534	0.9599	1.07	1.09	1.23	1.78
	2	0.9508	0.9515	0.9535	0.9587	1.07	1.09	1.23	1.78
	4	0.9510	0.9511	0.9544	0.9615	1.07	1.09	1.23	1.78
	8	0.9502	0.9508	0.9533	0.9596	1.07	1.09	1.23	1.78
50	1	0.9510	0.9526	0.9546	0.9607	1.06	1.08	1.22	1.77
	2	0.9503	0.9511	0.9537	0.9599	1.06	1.08	1.22	1.77
	4	0.9495	0.9517	0.9529	0.9598	1.06	1.08	1.22	1.77
	8	0.9516	0.9514	0.9536	0.9600	1.06	1.08	1.22	1.77
10	1	0.9505	0.9513	0.9531	0.9596	0.987	1.01	1.15	1.70
	2	0.9511	0.9522	0.9529	0.9590	0.987	1.01	1.15	1.70
	4	0.9511	0.9499	0.9522	0.9582	0.987	1.01	1.15	1.70
	8	0.9500	0.9509	0.9525	0.9580	0.987	1.01	1.15	1.70
5	1	0.9503	0.9514	0.9517	0.9569	0.831	0.850	0.984	1.48
	2	0.9496	0.9502	0.9526	0.9582	0.830	0.851	0.985	1.47
	4	0.9507	0.9492	0.9526	0.9576	0.830	0.851	0.985	1.48
	8	0.9518	0.9517	0.9512	0.9562	0.831	0.853	0.984	1.47
3	1	0.9514	0.9515	0.9515	0.9550	0.496	0.510	0.597	0.916
	2	0.9508	0.9499	0.9521	0.9554	0.496	0.509	0.598	0.919
	4	0.9508	0.9512	0.9506	0.9549	0.495	0.510	0.598	0.919
	8	0.9501	0.9501	0.9509	0.9539	0.496	0.509	0.595	0.918

Table 3. Observed success-rates for Bonferroni rectangles, calculated using equations (7) and (8), and the ratio of mean area to the mean area of elliptical regions. The uncertainty in success-rates as estimates of coverage probability is approximately 0.0014.

Table 3 shows the success-rates for uncertainty rectangles. The results indicate no less than nominal coverage probability is obtained in all cases, as expected. However, surprisingly, the mean area ratios become significantly less than unity when ν and ρ are both small. In other words, uncertainty rectangles are more informative than ellipses when there is little or no correlation between measurement errors and low degrees of freedom. This behaviour is due to the way that the coverage factors $k_{\mathrm{B}\cdot p}$ and $k_{\mathrm{ell}\cdot p}$

depend on ν. The ratio of rectangle to ellipse areas for a particular covariance matrix $\mathbf{v}$ is

$$\frac{4}{\pi}\left(\frac{k_{\mathrm{B}\cdot p}}{k_{\mathrm{ell}\cdot p}}\right)^2 \frac{1}{\sqrt{1-r^2}}\,,$$

where the correlation coefficient $r = \sqrt{(v_{12}v_{21})/(v_{11}v_{22})}$. With $p = 95\%$ and $\nu = 500$ the ratio

$$\frac{4}{\pi}\left(\frac{k_{\mathrm{B}\cdot p}}{k_{\mathrm{ell}\cdot p}}\right)^2 = 1.0655\,,$$

but that falls to 0.3896 when $\nu = 3$. So when measurement errors are only lightly correlated, the mean of $1/\sqrt{1-r^2}$ values generated during the simulations is not enough to compensate for this drop, and mean area ratios less than unity are observed.

5. Uncertainty parallelograms

Some information about uncertainty is ignored when constructing both uncertainty circles and uncertainty rectangles, which could impact on the performance of uncertainty calculations. So, we now consider the construction of parallelogrammatic uncertainty regions that use all covariance matrix elements in their construction.

There is a number of ways to construct a parallelogram that circumscribes an elliptical uncertainty region. In particular, one pair of sides may be chosen parallel to a coordinate axis (real or imaginary) and the other sides aligned parallel to an ellipse axis (see Fig. 2). Such a choice will simplify reporting, because the uncertainty of one component is represented by an interval centered on the measured value, while the uncertainty of the other component is represented by an interval located on a line parallel to one ellipse axis and passing through the measured value. The slope of that line depends on the correlation coefficient (or, equivalently, on v_{21}).

For an uncertainty parallelogram centered on $\boldsymbol{x}$, with a pair of sides parallel to the imaginary axis, a point $\boldsymbol{\xi}$ inside the region must satisfy both

$$|x_{\mathrm{re}} - \xi_{\mathrm{re}}| < U^{\sharp}_{\mathrm{re}} \tag{9}$$

and

$$\left|x_{\mathrm{im}} - \beta^{\sharp}(x_{\mathrm{re}} - \xi_{\mathrm{re}}) - \xi_{\mathrm{im}}\right| < U^{\sharp}_{\mathrm{im}}\,. \tag{10}$$

The constants $U^{\sharp}_{\mathrm{re}}$, $U^{\sharp}_{\mathrm{im}}$ depend on the covariance matrix elements and the coverage factor for an ellipse,

$$U^{\sharp}_{\mathrm{re}} = k_{\mathrm{ell},p}\,\sqrt{v_{11}}$$
$$U^{\sharp}_{\mathrm{im}} = k_{\mathrm{ell},p}\,\sqrt{v_{22} - v_{21}^2/v_{11}}$$
$$\beta^{\sharp} = \frac{v_{21}}{v_{11}}\,.$$

Similarly, for a parallelogram centered at $\boldsymbol{z}_0$, with a pair of sides parallel to the real axis, a point $\boldsymbol{\xi}$ inside the region must satisfy

$$\left|x_{\mathrm{re}} - \beta^{\flat}(x_{\mathrm{im}} - \xi_{\mathrm{im}}) - \xi_{\mathrm{re}}\right| < U^{\flat}_{\mathrm{re}} \tag{11}$$

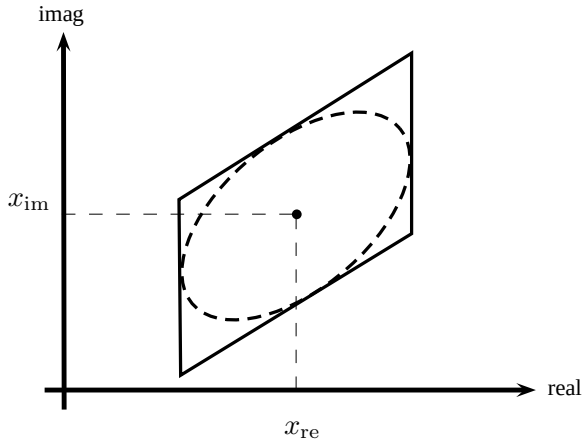

Figure 2. An uncertainty region constructed as a parallelogram with one pair of sides parallel to the imaginary coordinate axis. The conventional uncertainty ellipse is contained, ensuring that the coverage probability of the parallelogram is no less than nominal.

and

$$|x_{\rm im} - \xi_{\rm im}| < U^\flat_{\rm im} \tag{12}$$

where,

$$U^\flat_{\rm re} = k_{{\rm ell},p}\sqrt{v_{11} - v_{21}^2/v_{22}}$$
$$U^\flat_{\rm im} = k_{{\rm ell},p}\sqrt{v_{22}}$$
$$\beta^\flat = \frac{v_{21}}{v_{22}}\,.$$

5.1. Performance

Table 4 shows the observed coverage probabilities, and the mean area ratios, for parallelograms with one pair of sides parallel to the real axis. There was no apparent difference between this data and the results obtained for parallelograms constructed with a pair of sides parallel to the imaginary axis, so only one set of results is presented.

The coverage probability estimates are never less than nominal, as expected, because these regions enclose the corresponding uncertainty ellipses. However, it is interesting that the success-rates for a given ν appear to be independent of the covariance matrix $\mathbf{\Sigma}$. This suggests that there is a direct relationship between parallelogram coverage factor and the parameters ν and p, as is the case for elliptical regions. It is also notable that all the mean area ratios are constant. In fact, the parallelogram area (for either type of construction) is

$$4k_{{\rm ell},p}^2\sqrt{v_{11}v_{22} - v_{12}v_{21}}\,,$$

while the area of the enclosed uncertainty ellipse is

$$\pi k_{{\rm ell},p}^2\sqrt{v_{11}v_{22} - v_{12}v_{21}}\,,$$

so the ratio $4/\pi = 1.27$ is to be expected.

		success-rate				mean area ratio			
ν	l	$\rho = 0.0$	0.2	0.5	0.8	$\rho = 0.0$	0.2	0.5	0.8
500	1	0.9715	0.9713	0.9716	0.9720	1.27	1.27	1.27	1.27
	2	0.9713	0.9712	0.9716	0.9709	1.27	1.27	1.27	1.27
	4	0.9706	0.9714	0.9711	0.9714	1.27	1.27	1.27	1.27
	8	0.9717	0.9719	0.9710	0.9710	1.27	1.27	1.27	1.27
50	1	0.9712	0.9705	0.9702	0.9711	1.27	1.27	1.27	1.27
	2	0.9705	0.9709	0.9711	0.9698	1.27	1.27	1.27	1.27
	4	0.9710	0.9714	0.9709	0.9708	1.27	1.27	1.27	1.27
	8	0.9707	0.9708	0.9706	0.9703	1.27	1.27	1.27	1.27
10	1	0.9661	0.9667	0.9669	0.9657	1.27	1.27	1.27	1.27
	2	0.9658	0.9678	0.9662	0.9669	1.27	1.27	1.27	1.27
	4	0.9660	0.9672	0.9662	0.9669	1.27	1.27	1.27	1.27
	8	0.9662	0.9667	0.9659	0.9665	1.27	1.27	1.27	1.27
5	1	0.9610	0.9601	0.9608	0.9600	1.27	1.27	1.27	1.27
	2	0.9606	0.9603	0.9604	0.9603	1.27	1.27	1.27	1.27
	4	0.9595	0.9609	0.9617	0.9616	1.27	1.27	1.27	1.27
	8	0.9602	0.9597	0.9598	0.9612	1.27	1.27	1.27	1.27
3	1	0.9568	0.9552	0.9552	0.9542	1.27	1.27	1.27	1.27
	2	0.9550	0.9544	0.9543	0.9557	1.27	1.27	1.27	1.27
	4	0.9543	0.9548	0.9550	0.9548	1.27	1.27	1.27	1.27
	8	0.9544	0.9549	0.9547	0.9544	1.27	1.27	1.27	1.27

Table 4. Estimates of coverage probability for parallelograms constructed using equations (11) and (12), with sides parallel to the real coordinate axis, and the ratio of mean area to the mean area of an elliptical region. The uncertainty in these estimates of coverage probability is approximately 0.0014.

5.2. Improving performance

A simple numerical procedure has been used to chose coverage factors $k_{\mathrm{par},95}$, specific to the parallelogrammatic shape, for different values of ν. The procedure is described in Appendix A and the coverage factors obtained are reported in Table A1. Using these coverage factors to construct parallelogrammatic regions, in place of $k_{\mathrm{ell},p}$, the success-rates shown in Table 5 were obtained. The observed coverage probabilities are now effectively nominal and the mean area ratios are significantly reduced, indicating that the parallelogram areas are now only slightly bigger than the equivalent ellipses.

6. Discussion and conclusions

There does not appear to be a simple way to report the extent of an elliptical region representing the expanded uncertainty of a complex quantity. So, depending on the purpose of a measurement, the recipient of a report may find the alternative shapes

		success-rate				mean area ratio			
ν	l	$\rho = 0.0$	0.2	0.5	0.8	$\rho = 0.0$	0.2	0.5	0.8
500	1	0.9517	0.9498	0.9500	0.9504	1.06	1.06	1.06	1.06
	2	0.9497	0.9505	0.9505	0.9510	1.06	1.06	1.06	1.06
	4	0.9502	0.9496	0.9501	0.9499	1.06	1.06	1.06	1.06
	8	0.9504	0.9501	0.9493	0.9491	1.06	1.06	1.06	1.06
50	1	0.9497	0.9490	0.9502	0.9500	1.06	1.06	1.06	1.06
	2	0.9489	0.9510	0.9495	0.9486	1.06	1.06	1.06	1.06
	4	0.9496	0.9494	0.9506	0.9504	1.06	1.06	1.06	1.06
	8	0.9501	0.9496	0.9490	0.9485	1.06	1.06	1.06	1.06
10	1	0.9501	0.9500	0.9501	0.9485	1.06	1.06	1.06	1.06
	2	0.9498	0.9490	0.9488	0.9507	1.06	1.06	1.06	1.06
	4	0.9509	0.9499	0.9495	0.9512	1.06	1.06	1.06	1.06
	8	0.9496	0.9493	0.9489	0.9502	1.06	1.06	1.06	1.06
5	1	0.9508	0.9500	0.9495	0.9508	1.08	1.08	1.08	1.08
	2	0.9510	0.9501	0.9502	0.9505	1.08	1.08	1.08	1.08
	4	0.9490	0.9504	0.9508	0.9500	1.08	1.08	1.08	1.08
	8	0.9489	0.9495	0.9505	0.9513	1.08	1.08	1.08	1.08
3	1	0.9512	0.9492	0.9499	0.9489	1.14	1.14	1.14	1.14
	2	0.9492	0.9507	0.9494	0.9498	1.14	1.14	1.14	1.14
	4	0.9506	0.9506	0.9498	0.9505	1.14	1.14	1.14	1.14
	8	0.9496	0.9493	0.9502	0.9497	1.14	1.14	1.14	1.14

Table 5. Estimated coverage probabilities for the same parallelogrammatic constructions as reported in Table 4, but using the coverage factors reported in Table A1. The uncertainty in the estimates of coverage probability is approximately 0.0014.

discussed here more convenient.

As mentioned in the Introduction, there are several reasons why circular uncertainty regions may be appealing. Nevertheless, this study has found that they are not the bset choice when full covariance matrix information is available, or when the number of degrees of freedom is small. Circles do perform well over a narrow range of parameters but can also provide coverage probabilities significantly above or below nominal in most other cases. The observed coverage probabilities in this study varied from below 92% to above 99%.

Rectangular uncertainty regions are a better choice. The sides of a rectangular region can be reported as simultaneous uncertainty intervals for the real and imaginary components, which is easy to use when comparing measurement results. Uncertainty rectangles tend to be a little larger than the corresponding uncertainty ellipses under most conditions, and can become much larger when there is strong correlation between measurement errors. However, they can also become much smaller than ellipses when

there is little or no correlation between errors and degrees of freedom are low. For that reason, rectangular regions calculated using the Bonferroni coverage factor may be preferred when there is clear evidence that measurement errors in the real and imaginary components are independent.

The performance of parallelogrammatic uncertainty regions is consistent across the range of error conditions studied. When ν is high and correlation between errors is significant, parallelograms are the better choice and in the absence of strong correlation at high degrees of freedom, the difference in performance between rectangles and parallelograms is not significant. A format for reporting the extent of a parallelogrammatic region has been given that is concise and simple. So, these constructions offer a useful alternative to elliptical uncertainty regions. The table of parallelogrammatic coverage factors reported here, at a coverage probability of 95%, allows these regions to be constructed so that their areas are only slightly larger than the equivalent ellipses.

In conclusion, both a rectangular uncertainty region, with sides parallel to the real and imaginary component axes, and a parallelogrammatic uncertainty region, with a pair of sides parallel to one component axis, offer practical ways of reporting an expanded measurement uncertainty for complex quantities. On the other hand, the coverage probability of circular uncertainty regions varies by several percentage points above and below nominal, depending on the distribution of measurement errors and the number of degrees of freedom, and so this shape of uncertainty region is less satisfactory. The study found that parallelograms perform well over a broad range of conditions, while rectangular regions can produce smaller regions, and hence more informative results, in certain cases. The study also suggests that there are unique values for the coverage factor for parallelogrammatic regions that depend only on the degrees of freedom and desired coverage probability. Numerical estimates of the 95% coverage factors for parallelogrammatic regions have been tabulated.

Acknowledgement

The author would like to thank R Willink, for his comments and encouragement. The work was funded by the New Zealand Government as part of a contract for the provision of national measurement standards.

Appendix A. Estimated coverage factors for uncertainty parallelograms

The results obtained in §5.1 suggest that there is a unique coverage factor for parallelogrammatic uncertainty regions $k_{\text{par}\cdot p}$ that depends only on the degrees of freedom ν and the required coverage probability. A simple optimization procedure has been used here to estimate this coverage factor.

Varying the value of coverage factor used in the construction of parallelograms described in §5 gives rise to different success-rates in the simulations of §1.3. So, it is possible to search for a value that gives a success-rates close to 95%. We have done this for simulations using the same set of parameterizations of $\mathbf{\Sigma}$ ($l \in \{1.0, 2.0, 4.0, 8.0\}$ and $\rho \in \{0.0, 0.2, 0.5, 0.8\}$). For each value of ν, this produced 16 estimates of $k_{\text{par}\cdot 95}$ that varied slightly due to the randomness inherent in the simulation process. The mean of these 16 values is reported as $k_{\text{par}\cdot 95}$ in Table A1. The standard error *se* (the sample standard deviation divided by $\sqrt{16}$) is also reported.

ν	$k_{\text{par}\cdot 95}$	*se*	ν	$k_{\text{par}\cdot 95}$	*se*	ν	$k_{\text{par}\cdot 95}$	*se*
3	7.147	0.012	15	2.581	0.001	90	2.286	0.001
4	4.690	0.006	16	2.559	0.002	100	2.281	0.001
5	3.845	0.002	17	2.533	0.002	120	2.274	0.001
6	3.421	0.003	18	2.515	0.001	140	2.266	0.001
7	3.169	0.003	19	2.499	0.001	160	2.267	0.001
8	3.007	0.002	20	2.486	0.002	180	2.259	0.001
9	2.893	0.002	30	2.394	0.001	200	2.259	0.001
10	2.807	0.002	40	2.352	0.001	300	2.251	0.001
11	2.742	0.001	50	2.326	0.001	400	2.247	0.001
12	2.691	0.002	60	2.312	0.001	500	2.244	0.001
13	2.648	0.002	70	2.300	0.001	inf	2.236	0.001
14	2.613	0.001	80	2.293	0.001			

Table A1. Coverage factors for 95% parallelogrammatic uncertainty regions at different degrees of freedom ν. The parallelograms are constructed as described in §5. The column headed $k_{\text{par}\cdot 95}$ is the average of 16 values obtained for different l and ρ, the column headed *se* is the standard error of $k_{\text{par}\cdot 95}$.

References

[1] B D Hall. Expanded uncertainty regions for complex quantities in polar coordinates. (in preparation), 2013.

[2] Richard A. Johnson and Dean W. Wichern. *Applied multivariate statistical analysis*. Prentice-Hall International, 1998.

[3] N. M. Ridler and M. F. Salter. An approach to the treatment of uncertainty in complex S-parameter measurements. *Metrologia*, 39(3):295–302, June 2002.

[4] N M Ridler and C J Medley. An uncertainty budget for vhf and uhf reflectometers. DES Report 120, National Physical Laboratory, May 1992.

[5] BIPM, IEC, IFCC, ISO, IUPAC, IUPAP, and OIML. *Evaluation of measurement data ? Guide to the expression of uncertainty in measurement JCGM 100:2008 (GUM 1995 with minor corrections)*. BIPM Joint Committee for Guides in Metrology, Paris, Sèvres, 1 edition, 2008.

[6] Yu Song Meng and Yueyan Shan. Measurement uncertainty of complex-valued microwave quantities. *Progress in Electromagnetics Research*, 136:421–422, 2013.

[7] K. Yhland and J. Stenarson. A simplified treament of uncertainties in complex quantities. In *CPEM Conference Digest*, pages 652–653, 2004. (London, 2004).

[8] BIPM, IEC, IFCC, ISO, IUPAC, IUPAP, and OIML. *Evaluation of measurement data ? Supplement 2 to the "Guide to the expression of uncertainty in measurement" ? Extenstion to any number of output quantities JCGM 102:2011*. BIPM Joint Committee for Guides in Metrology, Paris, Sèvres, 1 edition, 2011.

[9] B. D. Hall. On the propagation of uncertainty in complex-valued quantities. *Metrologia*, 41(3):173–177, 2004.

[10] R Willink and B DHall. A classical method for uncertainty analysis with multidimensional data. *Metrologia*, 39:361–9, 2002.

[11] R. Willink. Principles of probability and statistics for metrology. *Metrologia*, 43:S211–S219, 2006.

[12] B. D. Hall. Using simulation to check uncertainty calculations. *Meas. Sci. Tech.*, 22(025105):10pp, 2011.